

DecAlign: Hierarchical Cross-Modal Alignment for Decoupled Multimodal Representation Learning

Chengxuan Qian¹, Shuo Xing¹, Shawn Li², Yue Zhao², Zhengzhong Tu^{1*}

¹ Texas A&M University ² University of Southern California

Abstract

Multimodal representation learning aims to capture both shared and complementary semantic information across multiple modalities. However, the intrinsic heterogeneity of diverse modalities presents substantial challenges to achieve effective cross-modal collaboration and integration. To address this, we introduce DecAlign, a novel hierarchical cross-modal alignment framework designed to decouple multimodal representations into modality-unique (heterogeneous) and modality-common (homogeneous) features. For handling heterogeneity, we employ a prototype-guided optimal transport alignment strategy leveraging gaussian mixture modeling and multi-marginal transport plans, thus mitigating distribution discrepancies while preserving modality-unique characteristics. To reinforce homogeneity, we ensure semantic consistency across modalities by aligning latent distribution matching with Maximum Mean Discrepancy regularization. Furthermore, we incorporate a multimodal transformer to enhance high-level semantic feature fusion, thereby further reducing cross-modal inconsistencies. Our extensive experiments on four widely used multimodal benchmarks demonstrate that DecAlign consistently outperforms existing state-of-the-art methods across five metrics. These results highlight the efficacy of DecAlign in enhancing superior cross-modal alignment and semantic consistency while preserving modality-unique features, marking a significant advancement in multimodal representation learning scenarios. Our project page is at <https://taco-group.github.io/DecAlign/> and the code is available at <https://github.com/taco-group/DecAlign>.

1. Introduction

Multimodal representation learning seeks to effectively harmonize diverse modalities by capturing their shared semantics while retaining modality-unique characteristics. This approach has achieved significant advances across various domains such as multimodal sentiment analysis [4, 18, 37], recommendation systems [23, 24], autonomous driving [13,

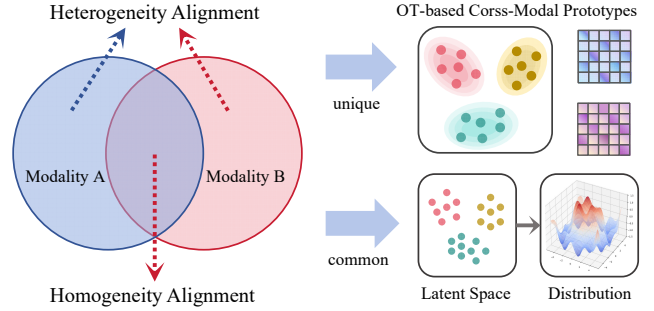


Figure 1. Overview of the proposed DecAlign framework, where multimodal representations capture both modality-unique characteristics and shared commonalities. By decoupling them into modality heterogeneity and homogeneity, followed by a hierarchical alignment strategy, we achieve seamless alignment from heterogeneous to homogeneous features.

26, 43, 44], out-of-distribution detection [5, 16], and large vision language models [38, 45, 56]. Despite these successes, the inherent modality heterogeneity—arising from distinct data distributions, representation scales, and semantic granularities—remains a significant barrier that limits their potential for seamless cross-modal collaboration.

This challenge is further intensified by the entanglement of modality-unique (heterogeneous) patterns and cross-modal common (homogeneous) semantics. Conventional multimodal fusion methods typically simplify the issue by projecting raw multimodal data into unified spaces via straightforward concatenation or linear transformations [10, 54]. However, this indiscriminate fusion entangles modality-unique features with shared semantics, leading to semantic interference, where detailed unimodal characteristics may disrupt global cross-modal relationships [19, 46]. This phenomenon is particularly evident when dealing with dimensional mismatches—such as high-dimensional, spatially correlated image features paired with low-dimensional, temporally correlated text features [40, 41, 58]. Such mismatches hinder effective cross-modal semantic alignment, causing potential information redundancy or loss during fusion.

To overcome these limitations, we propose DecAlign,

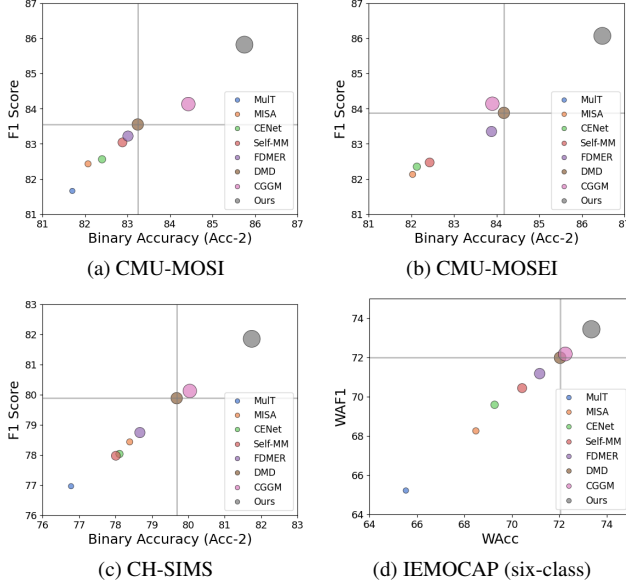


Figure 2. DecAlign achieves superior performance compared to state-of-the-art methods across multiple multimodal benchmarks. The bubble size represents relative model performance, illustrating the trade-off between Acc-2 and F1 Score.

a hierarchical cross-modal alignment framework for multimodal representation learning. As illustrated in Figure 1, DecAlign first explicitly decouple multimodal representations into modality-unique (heterogeneous) and modality-common (homogeneous) features through specialized encoders. Then, leveraging a dual-stream cross-modal alignment mechanism, DecAlign individually handles modality characteristics at different granularities: ❶ For heterogeneity, we propose prototype-based optimal transport alignment [28] using Gaussian Mixture Modeling (GMM) [2] and multi-marginal transport plans [27], effectively mitigating distribution discrepancies and constrain modality-unique interference. Furthermore, we incorporate a multimodal transformer module with cross-modal attention to align high-level semantics, bridges distribution gaps, reinforces discriminative representations, bridging semantic gaps across modalities. ❷ For homogeneity, DecAlign achieves semantic consistency via latent distribution matching and Maximum Mean Discrepancy (MMD) regularization. Finally, we concatenate the transformer-aligned modality-unique features with modality-common features, passing them through a learnable fully connected layer for downstream tasks. The key contributions of ourwork are summarized as follows:

- **Modality Decoupling.** We propose DecAlign, a novel hierarchical cross-modal alignment framework that decouples multimodal features into modality-heterogeneous and modality-homogeneous components, allowing tailored strategies to capture both modality-unique characteristics and shared semantics.

- **Hierarchical Alignment Strategy.** We develop a dual-stream alignment mechanism that combines prototype-guided optimal transport and cross-modal transformers to handle modality heterogeneity, while applying latent space statistical matching to address homogeneity, substantially improving cross-modal semantic integration.
- **Effectiveness.** Through comprehensive evaluation on four benchmark datasets, we demonstrate that DecAlign consistently surpasses state-of-the-art methods, confirming its efficacy for multimodal representation learning.

2. Related Work

2.1. Multimodal Representation Learning

Multimodal representation learning aims to integrate heterogeneous data from diverse modalities into a cohesive framework that captures complementary semantic information [1, 20, 29]. Recent methods have achieved significantly performance improvements by leveraging representation-based and cross-modal interaction approaches. Specifically, Self-MM [50] applies self-supervised contrastive learning and masked modeling to enhance the mutual information across modalities, HGraph-CL [22] introduces hierarchical graph contrastive learning to model intricate interactions across modalities. However, the heterogeneity and complementary information inherent in multimodal representations are intrinsically entangled, making it challenging to fully harness their complementary strengths while preserving their unique characteristics. Inspired by this insight, MISA [11] separates multimodal representations into modality-invariant and modality-unique features with contrastive and reconstruction losses, DMD [17] further introduces graph cross-modal knowledge distillation to explicitly model the correlations across modalities. However, existing methods are often constrained to modeling modalities from a global perspective, overlooking the token-level local semantic inconsistencies that arise in cross-modal interactions. Our proposed DecAlign enables fine-grained multimodal representation learning through hierarchical alignment, progressing from local to global and heterogeneity to homogeneity, ensuring precise cross-modal integration and semantic consistency.

2.2. Cross-Modal Alignment

The core challenge in multimodal tasks lies in the inherent heterogeneity across modalities [58], characterized by structural, distributional, and semantic disparities, which restricts the effective synergy of multimodal homogeneous features. To address this, existing solutions can be broadly categorized as follows: ❶ Shared Representation, which aims to learn a unified latent space for cross-modal semantic consistency. For example, CLIP-based methods [8, 30] use contrastive learning to align image-text pairs

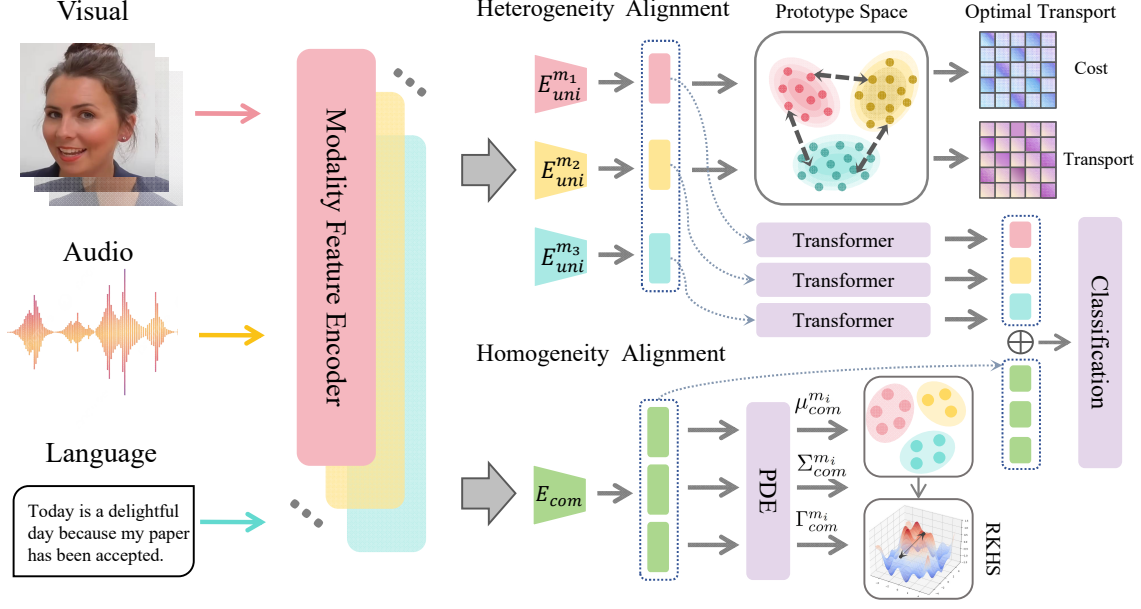


Figure 3. **The framework of our proposed DecAlign approach**, illustrated in a multimodal setting with visual, audio, and language inputs. Modality Feature Encoders first extract unimodal embeddings, which are then decoupled into modality heterogeneous and homogeneous components by modality-unique/common encoders. Heterogeneous features are aligned via optimal transport-based cross-modal prototypes, and homogeneous semantics are aligned through latent space semantics and Maximum Mean Discrepancy-based distribution matching. Heterogeneous features are refined by multimodal transformer for capturing finer-grained cross-modal interactions, then concatenated with homogeneous features and passed through a fully connected layer for downstream tasks.

in a shared embedding space, while Uni-Code [42] employs cross-modal information disentangling and exponential moving average to align semantically equivalent information in a shared latent space. ② Transformer-based methods that apply cross-attention to dynamically capture key information in cross-modal interactions [12, 35, 47]. ③ Modality Translation, which establishes mappings between modalities through cross-modal generation or reconstruction [25, 33, 53]. ④ Cross-Modal Knowledge Distillation, which addresses inter-modal contribution imbalances and explores cross-modal correlations. For example, DMD [17] employs graph distillation for dynamic knowledge transfer, and UMD [15] uses unified self-distillation to learn robust representations from consistent multimodal distributions. Unlike methods that overemphasize homogeneous information, we tackle the issue of over-alignment diminishing modality-unique characteristics through representation decoupling and a hierarchical alignment mechanism, ensuring cross-modal semantic consistency while retaining unimodal characteristics.

3. The Proposed Method

Motivation and Overview. The fundamental challenge in multimodal representation learning lies in effectively addressing the inherent conflicts between modality-unique characteristics and cross-modal semantic consistency. Two critical issues emerge: ① **Heterogeneity**: referring to in-

herent representation focus and distributional discrepancies among modalities that hinder cross-modal semantic alignment, ② **Homogeneity**: emphasizing the necessity of capturing shared semantics across modalities despite their inherent differences. To overcome these limitations, we propose DecAlign, a hierarchical cross-modal alignment framework that explicitly treats modality-unique and modality-common features with specific alignment strategies. As illustrated in Figure 3, DecAlign begins by decoupling multimodal representations into modality-unique (heterogeneous) and modality-common (homogeneous) features (Section 3.1). A hierarchical alignment mechanism is subsequently employed, combining prototype-guided multi-marginal optimal transport and cross-modal transformer for heterogeneous alignment (Section 3.2) and latent space semantic consistency with MMD regularization for homogeneous alignment (Section 3.3), ensuring the semantic consistency of modality-unique information and cross-modal commonality.

3.1. Multimodal Feature Decoupling

Given a multimodal dataset with M modalities, we first employ 1D temporal convolutional layers on unimodal features extracted from modality-unique encoders to aggregate temporal information. This shallow encoding process preserves the original temporal dimension while unifying the feature dimensions across modalities. The resulting unimodal fea-

tures are expressed as: $\tilde{\mathbf{X}}_m \in \mathbb{R}^{T_s \times d_s}$, where m denotes the modality index, T_m represents the temporal dimension, and d_m is the feature dimension of the corresponding modality.

The primary challenge in multimodal tasks lies in the inherent heterogeneity across modalities, hindering the integration of homogeneous features. To address this, we decouple the multimodal representations into **modality-common** features, which emphasize semantic consistency across modalities, and **modality-unique** features, capturing modality-unique characteristics with some redundancy. Building upon this, we employ three modality-unique encoders $\mathbf{E}_{\text{uni}}^{(m)}$ and a modality-shared encoder \mathbf{E}_{com} , to extract heterogeneous features as $\mathcal{F}_{\text{uni}}^{(m)} = \mathbf{E}_{\text{uni}}^{(m)}(\tilde{\mathbf{X}}_m)$ and cross-modal homogeneous features as $\mathcal{F}_{\text{com}} = \mathbf{E}_{\text{com}}(\tilde{\mathbf{X}}_m)$.

Considering the inherent heterogeneity and potential redundancy across modalities, we refine the decoupling process by clearly separating modality-unique and modality-common features. Instead of explicitly modeling distributions or computing mutual information which can significantly increase computational complexity, we use cosine similarity to quantify their potential overlap. Hence, the loss of decoupling process is formally defined as:

$$\mathcal{L}_{\text{dec}} = \sum_{m=1}^M \frac{\mathcal{F}_{\text{uni}}^{(m)} \cdot (\mathcal{F}_{\text{com}}^{(m)})^T}{\|\mathcal{F}_{\text{uni}}^{(m)}\| \|\mathcal{F}_{\text{com}}^{(m)}\|} \quad (1)$$

3.2. Heterogeneity Alignment

In multimodal tasks, modality-unique features encapsulate distinct characteristics inherent to each modality. However, differences in representation forms and distributions across modalities can result in semantic shifts during direct alignment, ultimately weakening the robustness of cross-modal alignment. To address this, we refine local alignment using category prototypes and leverage multi-marginal optimal transport-based dynamic transfer mechanism for adaptive, fine-grained feature alignment across modalities.

3.2.1. Prototype Generation

To flexibly capture the complex distributions and potential correlations in multimodal data, we employ the Gaussian Mixture Model (GMM), which leverages its soft assignment mechanism and Gaussian distribution assumption to more accurately represent the prototype structures of different modality features. We first model modality-unique features using GMM, with prototypes represented by the mean and covariance of Gaussian distributions:

$$\mathcal{P}_m = \{(\mu_m^1, \Sigma_m^1), (\mu_m^2, \Sigma_m^2), \dots, (\mu_m^K, \Sigma_m^K)\} \quad (2)$$

where K denotes the number of Gaussian Components, and μ_m^k, Σ_m^k represent the mean and covariance of the k -th Gaussian component for modality m , respectively. Then the

probability of n -th sample \mathbf{x}_n belonging to the k -th Gaussian component is calculated as:

$$w_m^n(k) = \frac{\pi_k \cdot \mathcal{N}(\mathbf{x}_m^n; \mu_m^k, \Sigma_m^k)}{\sum_{j=1}^K \pi_j \cdot \mathcal{N}(\mathbf{x}_m^n; \mu_m^j, \Sigma_m^j)} \quad (3)$$

π_k is the mixture coefficient of the k -th Gaussian component, and $\mathcal{N}(\mathbf{x}_m^i; \mu_m^k, \Sigma_m^k)$ is the probability density function of the Gaussian distribution:

$$\mathcal{N}(\mathbf{x}_m^i; \mu_m^k, \Sigma_m^k) = \frac{\exp(-\frac{1}{2}(\mathbf{x}_m^i - \mu_m^k)^T \Sigma_m^{k-1}(\mathbf{x}_m^i - \mu_m^k))}{(2\pi)^{d/2} |\Sigma_m^k|^{1/2}} \quad (4)$$

3.2.2. Prototype-guided Optimal Transport

The modality-unique features of different modalities often lie in distinct feature spaces with significant distributional differences, traditional point-to-point alignment methods struggle to capture both global and local relationships. To address this challenge in multimodal scenarios, we introduce a multi-marginal Optimal Transport approach to establish matches between distributions. The cross-modal prototype matching cost matrix is defined as:

$$C(k_1, k_2, \dots, k_M) = \sum_{1 \leq i \leq j \leq M} C_{i,j}(k_i, k_j) \quad (5)$$

where $C_{i,j}(k_i, k_j)$ represents the pairwise alignment cost between modalities m_i and m_j :

$$C_{i,j}(k_i, k_j) = \|\mu_i^{k_i} - \mu_j^{k_j}\|^2 + \text{Tr}(\Sigma_i^{k_i} + \Sigma_j^{k_j} - 2(\Sigma_i^{k_i} \Sigma_j^{k_j})^{\frac{1}{2}}) \quad (6)$$

The optimization objective for cross-modal prototype alignment aims to minimize the total alignment cost across all modalities while satisfying marginal distribution constraints. The objective function is defined as:

$$T^* = \arg \min_T \sum_k T(k) \cdot C(k) + \lambda \sum_k T(k) \log T(k) \quad (7)$$

where $k \in \{k_1, k_2, \dots, k_M\}$ denotes the set of indices spanning all prototype combinations across the M modalities, $T(k)$ represents the joint transportation matrix, and $C(k)$ is the joint cost matrix. The second term introduces entropy regularization to promote smoother and more robust solutions. The transport plan matrix $T(k)$ is further constrained to ensure consistency across modalities, satisfying the following marginal distribution constraints:

$$\sum_{k_j: j \neq i} T(k_1, k_2, \dots, k_M) = \nu_i(k_i), \forall i \in \{1, 2, \dots, M\}, \forall k_i \quad (8)$$

$\nu_i(j_i)$ represents the marginal distribution of modality m_i over its prototypes. Combining global alignment via Optimal Transport and local alignment through sample-to-prototype calibration, the overall heterogeneity alignment

loss is defined as:

$$\mathcal{L}_{hete} = \sum_k T^*(k) \cdot C(k) + \frac{1}{N} \sum_{n=1}^N \sum_{k=1}^K w_i^n(k) \cdot \|\mathcal{F}_i^n - \mu_{j \neq i}^k\|^2 \quad (9)$$

the first term, \mathcal{L}_{OT} aligns the distributions of prototypes across modalities, ensuring global consistency. The second term \mathcal{L}_{Proto} ensures fine-grained alignment by minimizing the weighted distance between samples x_i^n in source modality i and prototypes in target modality j . By combining \mathcal{L}_{OT} and \mathcal{L}_{Proto} , this heterogeneous alignment loss captures both global and local relationships, providing a robust mechanism for aligning heterogeneous modalities in a unified feature space.

3.3. Homogeneity Alignment

While different modalities exhibit unique characteristics in their representations, they also share common elements that convey the same semantic information. To effectively uncovering and aligning these shared features, it is crucial to address the inherent challenges posed by modality-unique variations and residual inconsistencies in their distributions.

3.3.1. Latent Space Semantic Alignment

To address the global offset and semantic inconsistencies in modality-common features and mitigate information distortion during feature fusion, we model modality feature distributions using Gaussian distributions. By mapping representations into a latent space, we quantify differences in position, shape, and symmetry through mean, covariance, and skewness. Specifically, for modality-common features, their distributions are approximated as $\mathcal{Z}_{com}^{m_i} \sim \mathcal{N}(\mu_{com}^{m_i}, \Sigma_{com}^{m_i}, \Gamma_{com}^{m_i})$, where $\mu_{com}^{m_i}$, $\Sigma_{com}^{m_i}$ and $\Gamma_{com}^{m_i}$ represent the mean, covariance and skewness of the common features for modality m_i , respectively. Their detailed formulas are discussed in the Appendix. To ensure semantic consistency across modalities, we define the latent space semantic alignment loss as:

$$\mathcal{L}_{sem} = \frac{1}{M(M-1)} \sum_{1 \leq i < j \leq M} \left(\|\mu_{com}^{m_i} - \mu_{com}^{m_j}\|^2 + \|\Sigma_{com}^{m_i} - \Sigma_{com}^{m_j}\|_F^2 + \|\Gamma_{com}^{m_i} - \Gamma_{com}^{m_j}\|^2 \right) \quad (10)$$

3.3.2. Cross-Modal Distribution Alignment

To flexibly model the latent distribution space of modality-homogeneous features extracted by the shared encoder without relying on prior knowledge, we employ Maximum Mean Discrepancy (MMD), which maps data to a high-dimensional space using kernel functions and computes the distance between their means, enabling non-parametric and distribution-agnostic modeling. The discrepancy of cross-

modal distribution is then quantified as:

$$\mathcal{L}_{MMD} = \frac{2}{M(M-1)} \sum_{1 \leq i < j \leq M} \left[\mathbb{E}_{x, x' \sim \mathcal{Z}_{com}^{m_i}} [k(x, x')] + \mathbb{E}_{y, y' \sim \mathcal{Z}_{com}^{m_j}} [k(y, y')] - 2 \mathbb{E}_{x \sim \mathcal{Z}_{com}^{m_i}, y \sim \mathcal{Z}_{com}^{m_j}} [k(x, y)] \right] \quad (11)$$

where $k(\cdot, \cdot)$ is the Gaussian kernel function defined with its kernel bandwidth parameter σ :

$$k(x, y) = \exp \left(-\frac{\|x - y\|^2}{2\sigma^2} \right) \quad (12)$$

By conducting latent space semantic alignment followed by MMD-based distribution correction, we establish a hierarchical homogeneity alignment mechanism that effectively achieves semantic and distributional consistency of modality-common features. The overall loss for homogeneity alignment is $\mathcal{L}_{homo} = \mathcal{L}_{sem} + \mathcal{L}_{MMD}$.

3.4. Multimodal Fusion and Prediction

Recognizing the unique characteristics of multimodal heterogeneous representations, such as syntactic structures in language, spatial relationships in vision, and temporal patterns in audio, we incorporate multimodal transformer [35] to model global temporal information, providing finer-grained and more consistent feature representations across modalities. These features are then fused with modality-common features via a concatenation operation and passed through a fully connected layer to produce the final prediction results. The overall optimization objective of our framework is defined as:

$$\mathcal{L}_{total} = \mathcal{L}_{task} + \mathcal{L}_{dec} + \alpha \mathcal{L}_{hete} + \beta \mathcal{L}_{homo} \quad (13)$$

where \mathcal{L}_{task} represents the task-specific loss, such as cross-entropy for classification tasks or mean squared error for regression. α and β are trade-off hyper-parameters for the losses of heterogeneous and homogeneous alignment, with their sensitivity analyzed in Section 4.3.

4. Experiments

Datasets. To ensure direct and fair comparison with prior works, we evaluate DecAlign on four widely used benchmarking datasets, all of which contain textual, visual, and acoustic modalities. CMU-MOSI [51] (2199 clips) and CMU-MOSEI [52] (22856 clips) provide word-aligned multimodal signals. Each sample is annotated with a sentiment score ranging from -3 (highly negative) to +3 (highly positive). CH-SIMS [49] includes 38,280 Chinese utterances with sentiment score ranging from -1 (negative) to +1 (positive). IEMOCAP [3] features 10,039 dynamic utterances annotated for six emotions: angry, happy, sad, neutral, excited, and frustrated.

Models	CMU-MOSI					CMU-MOSEI				
	MAE (\downarrow)	Corr (\uparrow)	Acc-2 (\uparrow)	Acc-7 (\uparrow)	F1 Score (\uparrow)	MAE (\downarrow)	Corr (\uparrow)	Acc-2 (\uparrow)	Acc-7 (\uparrow)	F1 Score (\uparrow)
MFM [34]	0.951	0.662	78.18	36.21	78.10	0.681	0.555	78.93	45.93	76.45
MuT [35]	0.846	0.725	81.70	40.05	81.66	0.673	0.677	80.85	48.37	80.86
PMR [6]	0.895	0.689	79.88	40.60	79.83	0.645	0.689	81.57	48.88	81.56
CubeMLP [31]	0.838	0.695	81.85	41.03	81.74	0.601	0.701	81.36	49.07	81.75
MUTA-Net [32]	0.767	0.736	82.12	40.88	82.07	0.617	0.717	81.76	49.88	82.01
MISA [11]	0.788	0.744	82.07	41.27	82.43	0.594	0.724	82.03	51.43	82.13
CENet [36]	0.745	0.749	82.40	41.32	82.56	0.588	0.738	82.13	52.31	82.35
Self-MM [50]	0.765	0.764	82.88	42.03	83.04	0.576	0.732	82.43	52.68	82.47
FDMER [47]	0.760	0.777	83.01	42.88	83.22	0.571	0.743	83.88	53.21	83.35
AOBERT [14]	0.780	0.773	83.03	43.21	83.02	0.588	0.738	83.90	52.47	83.14
DMD [17]	<u>0.744</u>	0.788	83.24	<u>43.88</u>	83.55	0.561	0.758	84.17	<u>54.18</u>	83.88
MCIS [48]	0.756	0.783	84.02	43.58	83.85	<u>0.557</u>	0.747	<u>84.97</u>	53.85	<u>84.34</u>
CGGM [9]	0.747	<u>0.798</u>	<u>84.43</u>	43.21	<u>84.13</u>	0.551	<u>0.761</u>	83.90	53.47	84.14
DecAlign (Ours)	0.735	0.811	85.75	45.07	85.82	0.543	0.768	86.48	55.02	86.07

Table 1. Performance Comparison on CMU-MOSI and CMU-MOSEI datasets. \uparrow and \downarrow indicate that higher or lower value is better. Best results are highlighted in **bold**, and suboptimal results are underlined.

Evaluation Metrics. For CMU-MOSI and CMU-MOSEI, following prior works [17, 21, 57], we evaluate performance using binary accuracy (Acc-2), 7-class accuracy (Acc-7), and Binary F1 Score. Acc-2 reflects whether the a sample is predicted as negative, while sentiment intensity prediction is further assessed via Mean Absolute Error (MAE) and Pearson Correlation (Corr) to capture deviation and linearity. For CH-SIMS, we adopt MAE and F1 Score. IEMOCAP follows [7, 18, 55] with weighted accuracy (WAcc) and weighted average F1 Score (WAF1), accounting for class distribution imbalance.

Implementation Details. Consistent with previous studies [17, 39], we apply MMSA-FET Toolkit [49, 50] to extract features except for IEMOCAP dataset. For IEMOCAP, we follow prior work [18] for pre-processing. We adopt Adam as optimizer and implement all the experiments on an NVIDIA A6000 ADA with 48 GB memory. Pre-processing details and configuration settings are listed in Appendix.

4.1. Comparison with State-of-the-art Methods

We compare our DecAlign approach with state-of-the-art methods under unified environmental and dataset settings: MFM [34], MuT [35], PMR [6], CubeMLP [31], MUTA-Net [32], MISA [11], CENet [36], Self-MM [50], FDMER [47], AOBERT [14], DMD [17], MCIS [48], and CGGM [9]. Table 1 & 2, along with Figure 2, presents a comprehensive comparison of our proposed DecAlign framework against state-of-the-art methods on four datasets, evaluated across five metrics which jointly assess the model’s performance from both regression and classification perspectives. The results demonstrate that DecAlign consistently outperforms all baselines, achieving the lowest MAE and highest Corr, indicating superior performance in sentiment intensity estimation, as well as the highest classification accuracy across Acc-2, Acc-7, and F1 Score, confirming its ability to

Models	CH-SIMS		IEMOCAP (six-class)	
	MAE (\downarrow)	F1 Score (\uparrow)	WAcc (\uparrow)	WAF1 (\uparrow)
MFM [34]	0.471	75.28	63.38	63.41
MuT [35]	0.455	76.96	65.53	65.21
PMR [6]	0.445	76.55	67.04	67.01
CubeMLP [31]	0.459	77.85	66.43	66.41
MUTA-Net [32]	0.443	77.21	67.44	68.78
MISA [11]	0.437	78.43	68.48	68.25
CENet [36]	0.454	78.03	69.27	69.58
Self-MM [50]	0.432	77.97	70.35	70.43
FDMER [47]	0.424	78.74	71.33	71.17
AOBERT [14]	0.430	78.55	71.04	70.89
DMD [17]	0.421	79.88	72.03	71.98
MCIS [48]	0.429	79.58	71.77	71.53
CGGM [9]	<u>0.417</u>	<u>80.12</u>	<u>72.25</u>	<u>72.17</u>
DecAlign (Ours)	0.403	81.85	73.35	73.43

Table 2. Performance comparison on CH-SIMS and IEMOCAP datasets. \uparrow indicates that higher values are better. Best results are highlighted in **bold**, and runner-up results are underlined.

capture both fine-grained and high-level semantic patterns. **Transformer-based methods.** Compared to Transformer-based methods such as MuT [35], Self-MM [50], PMR [6], and MUTA-Net [32], which rely on cross-attention mechanism for global feature fusion, DecAlign overcomes modality-unique interference and local semantic inconsistencies. Transformer-based models assume a shared latent space, often causing dominant modalities to overshadow weaker ones, leading to information loss. In contrast, DecAlign explicitly disentangles modality-heterogeneous and modality-homogeneous features, leveraging prototype-based optimal transport for fine-grained alignment and latent space semantic alignment with MMD regularization for global consistency. This mitigates modality interference, reducing MAE and improving Corr, while enhancing classification performance.

Feature Decoupling-based methods. While multimodal feature decoupling methods such as MISA [11], FDMER

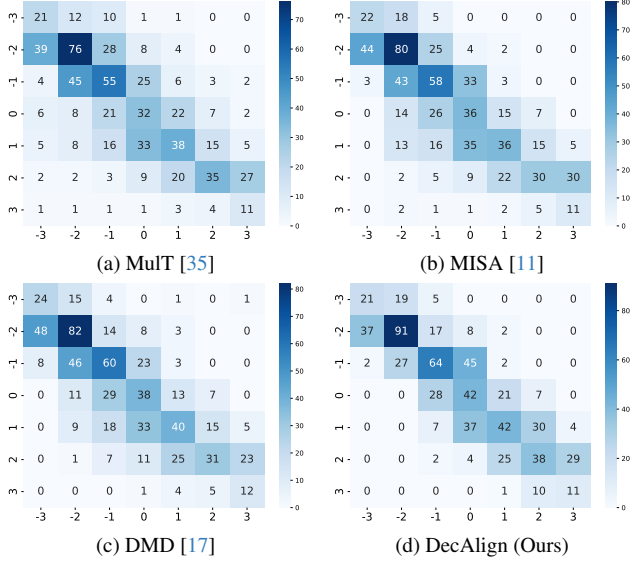


Figure 4. Confusion matrix comparison with state-of-the-art methods, illustrating the distribution of predicted sentiment categories against ground truth labels on the CMU-MOSI dataset.

Modules			CMU-MOSI		CMU-MOSEI	
MFD	Hete	Homo	MAE	F1 Score	MAE	F1 Score
✓	✓	✗	0.747	84.46	0.562	84.74
✓	✗	✓	0.754	84.03	0.588	84.37
✓	✗	✗	0.784	81.92	0.632	82.22
✗	✗	✗	0.794	81.56	0.624	81.87

Table 3. Ablation study on different key modules for CMU-MOSI and CMU-MOSEI datasets.

Modules				CMU-MOSI		CMU-MOSEI	
Proto-OT	CT	Sem	MMD	MAE	F1 Score	MAE	F1 Score
✓	✓	✓	✗	0.741	84.61	0.564	85.26
✓	✓	✗	✓	0.738	84.73	0.553	85.33
✓	✗	✓	✓	0.743	84.36	0.619	85.21
✗	✓	✓	✓	0.748	84.17	0.624	85.03

Table 4. Ablation study on different alignment strategies for CMU-MOSI and CMU-MOSEI datasets.

[47], and DMD [17] alleviate modality interference, they primarily focus on global alignment, often overlooking token-level inconsistencies. This limitation hinders fine-grained multimodal integration, particularly in tasks requiring precise semantic fusion. DecAlign overcomes this challenge through a dual-stream hierarchical alignment strategy, integrating prototype-based transport for local alignment with semantic consistency constraints for robust global integration. This enables more expressive multimodal representations, leading to superior performance across both regression and classification metrics.

Confusion Matrix Analysis. To further demonstrate the superiority of our performance and validate the effective-

ness of our proposed approach, we analyze the confusion matrix of DecAlign in comparison with representative works in the field of multimodal sentiment analysis, including MulT [35], MISA [11], and DMD [17]. As shown in Figure 4, DecAlign achieves a more balanced and accurate sentiment classification across different sentiment intensity levels, significantly reducing misidentification errors, particularly in distinguishing subtle sentiment variations.

Compared to other methods, DecAlign exhibits stronger diagonal dominance, reflecting higher sentiment classification accuracy. Notably, in extreme sentiment classes (-3 and +3), where existing models often misclassify samples, DecAlign significantly reduces confusion with adjacent sentiment levels. The higher concentration of correctly predicted samples in moderate sentiment categories (-1, 0, and 1) further demonstrates its ability to capture fine-grained sentiment distinctions, mitigating bias toward neutral or extreme labels. Furthermore, unlike MulT, MISA, and DMD, which struggle with negative-to-neutral misidentification, DecAlign achieves clearer separation between sentiment classes, ensuring more robust and interpretable predictions. This improvement is particularly evident in -2 and +2 classes, where DecAlign minimizes misidentification into adjacent categories, validating the effectiveness of its hierarchical alignment strategy in capturing both modality-unique nuances and shared semantic patterns.

4.2. Ablation Studies

To further evaluate the contributions of individual components in DecAlign, we conduct ablation studies on the MOSI and MOSEI dataset, while results on other benchmarks are given in the Appendix. The first study examines the impact of key model components, while the second focuses on the effectiveness of specific alignment strategies.

Impact of key components. We evaluate the impact of Multimodal Feature Decoupling (MFD), Heterogeneous (Hete), and Homogeneous (Homo) Alignment on model performance using MAE, Acc-2, and F1 Score (Table 3). The full model achieves the best results, confirming the significance of hierarchical alignment. Removing Homogeneous Alignment slightly increases MAE and lowers Acc-2, indicating the importance of intra-modal consistency. Eliminating Heterogeneous Alignment leads to a greater drop, showing that modality-unique interference affects feature integration. The absence of both alignments causes substantial performance degradation, highlighting the need to disentangle modality-homogeneous and modality-heterogeneous features.

Additionally, Figure 5 visualizes the ablation results across different sentiment categories, illustrating the performance variations when heterogeneous and homogeneous alignment modules are frozen. The degradation across sentiment categories further validates the necessity of a hier-

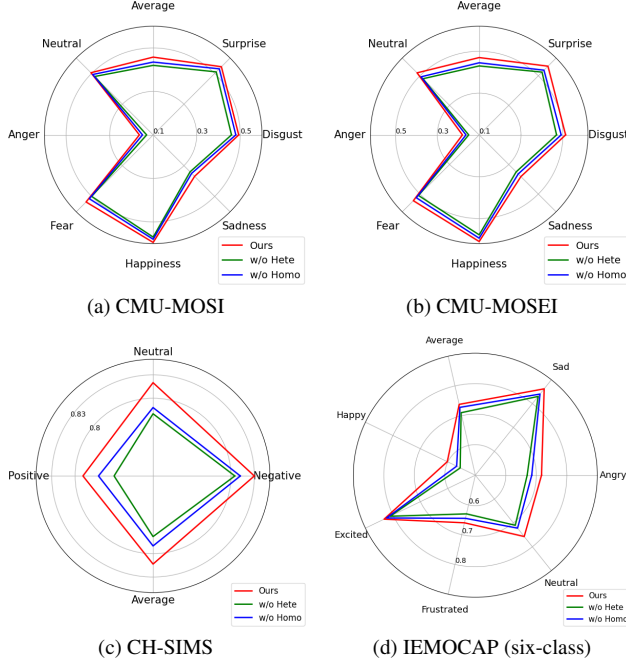


Figure 5. Visualization of ablation studies on accuracy comparison across different emotion categories.

archical alignment strategy to maintain robust performance across diverse emotional expressions. Notably, even when any single alignment module is disabled, the F1 Score remains higher than many state-of-the-art methods, including FDMER, AOBERT, and DMD, demonstrating the effectiveness of our proposed alignment approach from both heterogeneous and homogeneous perspectives. The most severe performance degradation occurs when MFD is removed, demonstrating that preserving modality-unique information before fusion is crucial. This underscores the effectiveness of integrating heterogeneous and homogeneous representations for better sentiment analysis.

Impact of specific alignment strategies. We further evaluate the contribution of Prototype-Based Optimal Transport (Proto-OT), Contrastive Training (CT), Semantic Consistency (Sem), and Maximum Mean Discrepancy (MMD) Regularization to DecAlign’s performance, as shown in Table 4. Removing MMD regularization leads to a slight performance drop, highlighting its role in global latent space alignment and feature coherence. The exclusion of semantic consistency further degrades performance, indicating that enforcing semantic alignment enhances multimodal feature integration. The most substantial drop occurs when contrastive training is removed, showing its critical role in learning discriminative multimodal representations. Similarly, eliminating Proto-OT results in a notable decline in both regression and classification metrics, demonstrating that fine-grained alignment through optimal transport significantly improves multimodal fusion and overall sentiment prediction accuracy.

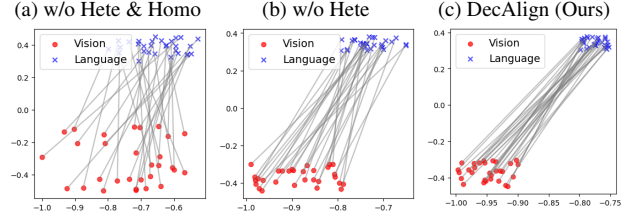


Figure 6. Visualization of the modality gap between vision and language on CMU-MOSEI dataset.

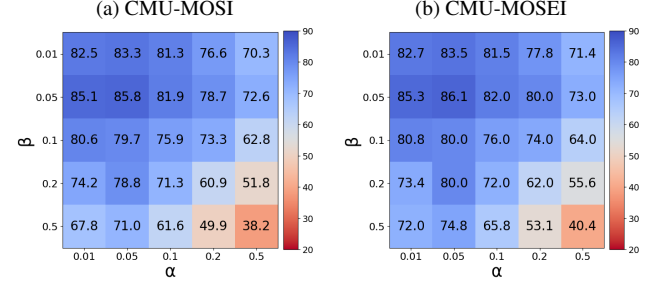


Figure 7. Hyperparameter sensitivity analysis on CMU-MOSI and CMU-MOSEI datasets in terms of Binary F1 Score.

Analysis of modality Gap. Figure 6 presents a case study on vision and language modalities, demonstrating how DecAlign mitigates the modality gap to enhance alignment. Models without heterogeneous or homogeneous alignment exhibit significantly larger gaps, hindering cross-modal fusion. These results further validate the effectiveness of our hierarchical alignment strategy.

4.3. Parameter Sensitivity Analysis

To analyze the impact of hyper-parameters α and β on the performance of DecAlign, we conduct an extensive grid search and evaluate the model’s Binary F1 Score across different parameter settings on MOSI and MOSEI datasets. Figure 7 presents a heatmap visualization of the results, where darker shades indicate higher performance. The optimal setting is $\alpha = 0.05, \beta = 0.05$, achieving the highest Performance across both datasets. Larger values cause a sharp performance drop, indicating that excessive alignment constraints hinder effective fusion. Smaller α values with moderate β yield strong performance, highlighting the importance of balancing prototype-based alignment and semantic consistency for optimal multimodal learning.

5. Conclusion and Further Discussion

Future work will integrate DecAlign with large multimodal pre-trained models (MLLMs) for fine-grained modality alignment at scale. This demands adaptive mechanisms to prevent modality collapse and enhance feature fusion efficiency, ensuring scalable and robust multimodal learning.

References

- [1] Khaled Bayouddh. A survey of multimodal hybrid deep learning for computer vision: Architectures, applications, trends, and challenges. *Information Fusion*, 105:102217, 2024. [2](#)
- [2] Christopher M Bishop. *Pattern Recognition and Machine Learning*. Springer, 2006. [2](#)
- [3] Carlos Busso, Murtaza Bulut, Chi-Chun Lee, Abe Kazemzadeh, Emily Mower, Samuel Kim, Jeannette N Chang, Sungbok Lee, and Shrikanth S Narayanan. Iemocap: Interactive emotional dyadic motion capture database. *Language resources and evaluation*, 42:335–359, 2008. [5](#)
- [4] Ringki Das and Thoudam Doren Singh. Multimodal sentiment analysis: a survey of methods, trends, and challenges. *ACM Computing Surveys*, 55(13s):1–38, 2023. [1](#)
- [5] Hao Dong, Yue Zhao, Eleni Chatzi, and Olga Fink. Multitood: Scaling out-of-distribution detection for multiple modalities. *Advances in Neural Information Processing Systems*, 37, 2024. [1](#)
- [6] Yunfeng Fan, Wenchao Xu, Haozhao Wang, Junxiao Wang, and Song Guo. Pmr: Prototypical modal rebalance for multimodal learning. In *Proceedings of the IEEE/CVF Conference on Computer Vision and Pattern Recognition*, pages 20029–20038, 2023. [6](#)
- [7] Fangze Fu, Wei Ai, Fan Yang, Yuntao Shou, Tao Meng, and Keqin Li. Sdr-gnn: Spectral domain reconstruction graph neural network for incomplete multimodal learning in conversational emotion recognition. *Knowledge-Based Systems*, page 112825, 2024. [6](#)
- [8] Peng Gao, Shijie Geng, Renrui Zhang, Teli Ma, Rongyao Fang, Yongfeng Zhang, Hongsheng Li, and Yu Qiao. Clip-adapter: Better vision-language models with feature adapters. *International Journal of Computer Vision*, 132(2): 581–595, 2024. [2](#)
- [9] Zirun Guo, Tao Jin, Jingyuan Chen, and Zhou Zhao. Classifier-guided gradient modulation for enhanced multimodal learning. *Advances in Neural Information Processing Systems*, 37:133328–133344, 2025. [6](#)
- [10] Zongbo Han, Fan Yang, Junzhou Huang, Changqing Zhang, and Jianhua Yao. Multimodal dynamics: Dynamical fusion for trustworthy multimodal classification. In *Proceedings of the IEEE/CVF conference on computer vision and pattern recognition*, pages 20707–20717, 2022. [1](#)
- [11] Devamanyu Hazarika, Roger Zimmermann, and Soujanya Poria. Misa: Modality-invariant and-specific representations for multimodal sentiment analysis. In *Proceedings of the 28th ACM international conference on multimedia*, pages 1122–1131, 2020. [2](#), [6](#), [7](#)
- [12] Zhangfeng Hu, Wenming Zheng, Yuan Zong, Mengting Wei, Xingxun Jiang, and Mengxin Shi. A novel decoupled prototype completion network for incomplete multimodal emotion recognition. In *2024 IEEE International Conference on Multimedia and Expo (ICME)*, pages 1–6. IEEE, 2024. [3](#)
- [13] Jyh-Jing Hwang, Runsheng Xu, Hubert Lin, Wei-Chih Hung, Jingwei Ji, Kristy Choi, Di Huang, Tong He, Paul Covington, Benjamin Sapp, et al. Emma: End-to-end multimodal model for autonomous driving. *arXiv preprint arXiv:2410.23262*, 2024. [1](#)
- [14] Kyeonghun Kim and Sanghyun Park. Aobert: All-modalities-in-one bert for multimodal sentiment analysis. *Information Fusion*, 92:37–45, 2023. [6](#)
- [15] Mingcheng Li, Dingkan Yang, Yuxuan Lei, Shunli Wang, Shuaibing Wang, Liuzhen Su, Kun Yang, Yuzheng Wang, Mingyang Sun, and Lihua Zhang. A unified self-distillation framework for multimodal sentiment analysis with uncertain missing modalities. In *Proceedings of the AAAI Conference on Artificial Intelligence*, pages 10074–10082, 2024. [3](#)
- [16] Shawn Li, Huixian Gong, Hao Dong, Tiankai Yang, Zhengzhong Tu, and Yue Zhao. Dpu: Dynamic prototype updating for multimodal out-of-distribution detection. *arXiv preprint arXiv:2411.08227*, 2024. [1](#)
- [17] Yong Li, Yuanzhi Wang, and Zhen Cui. Decoupled multimodal distilling for emotion recognition. In *Proceedings of the IEEE/CVF Conference on Computer Vision and Pattern Recognition*, pages 6631–6640, 2023. [2](#), [3](#), [6](#), [7](#)
- [18] Zheng Lian, Lan Chen, Licai Sun, Bin Liu, and Jianhua Tao. Gcnet: Graph completion network for incomplete multimodal learning in conversation. *IEEE Transactions on pattern analysis and machine intelligence*, 45(7):8419–8432, 2023. [1](#), [6](#)
- [19] Paul Pu Liang, Yun Cheng, Xiang Fan, Chun Kai Ling, Suzanne Nie, Richard Chen, Zihao Deng, Nicholas Allen, Randy Auerbach, Faisal Mahmood, et al. Quantifying & modeling multimodal interactions: An information decomposition framework. *Advances in Neural Information Processing Systems*, 36, 2024. [1](#)
- [20] Paul Pu Liang, Amir Zadeh, and Louis-Philippe Morency. Foundations & trends in multimodal machine learning: Principles, challenges, and open questions. *ACM Computing Surveys*, 56(10):1–42, 2024. [2](#)
- [21] Tao Liang, Guosheng Lin, Lei Feng, Yan Zhang, and Feng-mao Lv. Attention is not enough: Mitigating the distribution discrepancy in asynchronous multimodal sequence fusion. In *Proceedings of the IEEE/CVF International Conference on Computer Vision*, pages 8148–8156, 2021. [6](#)
- [22] Zijie Lin, Bin Liang, Yunfei Long, Yixue Dang, Min Yang, Min Zhang, and Ruifeng Xu. Modeling intra-and inter-modal relations: Hierarchical graph contrastive learning for multimodal sentiment analysis. In *Proceedings of the 29th International Conference on Computational Linguistics*, pages 7124–7135. Association for Computational Linguistics, 2022. [2](#)
- [23] Fan Liu, Huilin Chen, Zhiyong Cheng, Anan Liu, Liqiang Nie, and Mohan Kankanhalli. Disentangled multimodal representation learning for recommendation. *IEEE Transactions on Multimedia*, 25:7149–7159, 2022. [1](#)
- [24] Qijiong Liu, Jieming Zhu, Yanting Yang, Quanyu Dai, Zhaocheng Du, Xiao-Ming Wu, Zhou Zhao, Rui Zhang, and Zhenhua Dong. Multimodal pretraining, adaptation, and generation for recommendation: A survey. In *Proceedings of the 30th ACM SIGKDD Conference on Knowledge Discovery and Data Mining*, pages 6566–6576, 2024. [1](#)
- [25] Zhizhong Liu, Bin Zhou, Dianhui Chu, Yuhang Sun, and Lingqiang Meng. Modality translation-based multimodal sentiment analysis under uncertain missing modalities. *Information Fusion*, 101:101973, 2024. [3](#)

- [26] Yingzi Ma, Yulong Cao, Jiachen Sun, Marco Pavone, and Chaowei Xiao. Dolphins: Multimodal language model for driving. In *European Conference on Computer Vision*, pages 403–420. Springer, 2025. 1
- [27] Brendan Pass. Multi-marginal optimal transport: theory and applications. *ESAIM: Mathematical Modelling and Numerical Analysis*, 49(6):1771–1790, 2015. 2
- [28] Gabriel Peyré and Marco Cuturi. Computational optimal transport: With applications to data science. *Foundations and Trends in Machine Learning*, 11(5-6):355–607, 2019. 2
- [29] Chengxuan Qian, Kai Han, Jingchao Wang, Zhenlong Yuan, Rui Qian, Chongwen Lyu, Jun Chen, and Zhe Liu. Dyncim: Dynamic curriculum for imbalanced multimodal learning. *arXiv preprint arXiv:2503.06456*, 2025. 2
- [30] Alec Radford, Jong Wook Kim, Chris Hallacy, Aditya Ramesh, Gabriel Goh, Sandhini Agarwal, Girish Sastry, Amanda Askell, Pamela Mishkin, Jack Clark, et al. Learning transferable visual models from natural language supervision. In *International conference on machine learning*, pages 8748–8763. PMLR, 2021. 2
- [31] Hao Sun, Hongyi Wang, Jiaqing Liu, Yen-Wei Chen, and Lanfen Lin. Cubemlp: An mlp-based model for multimodal sentiment analysis and depression estimation. In *Proceedings of the 30th ACM international conference on multimedia*, pages 3722–3729, 2022. 6
- [32] Zemin Tang, Qi Xiao, Xu Zhou, Yangfan Li, Cen Chen, and Kenli Li. Learning discriminative multi-relation representations for multimodal sentiment analysis. *Information Sciences*, 641:119125, 2023. 6
- [33] Jialin Tian, Kai Wang, Xing Xu, Zuo Cao, Fumin Shen, and Heng Tao Shen. Multimodal disentanglement variational autoencoders for zero-shot cross-modal retrieval. In *Proceedings of the 45th International ACM SIGIR Conference on Research and Development in Information Retrieval*, pages 960–969, 2022. 3
- [34] Yao-Hung Hubert Tsai, Paul Pu Liang, Amir Zadeh, Louis-Philippe Morency, and Ruslan Salakhutdinov. Learning factorized multimodal representations. *arXiv preprint arXiv:1806.06176*, 2018. 6
- [35] Yao-Hung Hubert Tsai, Shaojie Bai, Paul Pu Liang, J Zico Kolter, Louis-Philippe Morency, and Ruslan Salakhutdinov. Multimodal transformer for unaligned multimodal language sequences. In *Proceedings of the 57th Annual Meeting of the Association for Computational Linguistics*, pages 6558–6569, 2019. 3, 5, 6, 7
- [36] Di Wang, Shuai Liu, Quan Wang, Yumin Tian, Lihuo He, and Xinbo Gao. Cross-modal enhancement network for multimodal sentiment analysis. *IEEE Transactions on Multimedia*, 25:4909–4921, 2022. 6
- [37] Lan Wang, Junjie Peng, Cangzhi Zheng, Tong Zhao, et al. A cross modal hierarchical fusion multimodal sentiment analysis method based on multi-task learning. *Information Processing & Management*, 61(3):103675, 2024. 1
- [38] Xiyao Wang, Jiuhai Chen, Zhaoyang Wang, Yuhang Zhou, Yiyang Zhou, Huaxiu Yao, Tianyi Zhou, Tom Goldstein, Parminder Bhatia, Furong Huang, et al. Enhancing visual-language modality alignment in large vision language models via self-improvement. *arXiv preprint arXiv:2405.15973*, 2024. 1
- [39] Yuanzhi Wang, Zhen Cui, and Yong Li. Distribution-consistent modal recovering for incomplete multimodal learning. In *Proceedings of the IEEE/CVF International Conference on Computer Vision*, pages 22025–22034, 2023. 6
- [40] Yake Wei, Di Hu, Henghui Du, and Ji-Rong Wen. On-the-fly modulation for balanced multimodal learning. *IEEE Transactions on Pattern Analysis and Machine Intelligence*, 2024. 1
- [41] Yake Wei, Siwei Li, Ruoxuan Feng, and Di Hu. Diagnosing and re-learning for balanced multimodal learning. In *European Conference on Computer Vision*, pages 71–86. Springer, 2025. 1
- [42] Yan Xia, Hai Huang, Jieming Zhu, and Zhou Zhao. Achieving cross modal generalization with multimodal unified representation. *Advances in Neural Information Processing Systems*, 36, 2024. 3
- [43] Shuo Xing, Hongyuan Hua, Xiangbo Gao, Shenzhe Zhu, Renjie Li, Kexin Tian, Xiaopeng Li, Heng Huang, Tianbao Yang, Zhangyang Wang, et al. Autotrust: Benchmarking trustworthiness in large vision language models for autonomous driving. *arXiv preprint arXiv:2412.15206*, 2024. 1
- [44] Shuo Xing, Chengyuan Qian, Yuping Wang, Hongyuan Hua, Kexin Tian, Yang Zhou, and Zhengzhong Tu. Openemmas: Open-source multimodal model for end-to-end autonomous driving. *arXiv preprint arXiv:2412.15208*, 2024. 1
- [45] Shuo Xing, Yuping Wang, Peiran Li, Ruizheng Bai, Yueqi Wang, Chengxuan Qian, Huaxiu Yao, and Zhengzhong Tu. Re-align: Aligning vision language models via retrieval-augmented direct preference optimization. *arXiv preprint arXiv:2502.13146*, 2025. 1
- [46] Peng Xu, Xiatian Zhu, and David A Clifton. Multimodal learning with transformers: A survey. *IEEE Transactions on Pattern Analysis and Machine Intelligence*, 45(10):12113–12132, 2023. 1
- [47] Dingkan Yang, Shuai Huang, Haopeng Kuang, Yangtao Du, and Lihua Zhang. Disentangled representation learning for multimodal emotion recognition. In *Proceedings of the 30th ACM International Conference on Multimedia*, pages 1642–1651, 2022. 3, 6, 7
- [48] Dingkan Yang, Mingcheng Li, Dongling Xiao, Yang Liu, Kun Yang, Zhaoyu Chen, Yuzheng Wang, Peng Zhai, Ke Li, and Lihua Zhang. Towards multimodal sentiment analysis debiasing via bias purification. In *European Conference on Computer Vision*, pages 464–481. Springer, 2024. 6
- [49] Wenmeng Yu, Hua Xu, Fanyang Meng, Yilin Zhu, Yixiao Ma, Jiele Wu, Jiyun Zou, and Kaicheng Yang. Ch-sims: A chinese multimodal sentiment analysis dataset with fine-grained annotation of modality. In *Proceedings of the 58th Annual Meeting of the Association for Computational Linguistics*, pages 3718–3727, 2020. 5, 6
- [50] Wenmeng Yu, Hua Xu, Ziqi Yuan, and Jiele Wu. Learning modality-specific representations with self-supervised multi-task learning for multimodal sentiment analysis. In *Proceed-*

ings of the AAAI conference on artificial intelligence, pages 10790–10797, 2021. [2](#), [6](#)

- [51] Amir Zadeh, Rowan Zellers, Eli Pincus, and Louis-Philippe Morency. Multimodal sentiment intensity analysis in videos: Facial gestures and verbal messages. *IEEE Intelligent Systems*, 31(6):82–88, 2016. [5](#)
- [52] AmirAli Bagher Zadeh, Paul Pu Liang, Soujanya Poria, Erik Cambria, and Louis-Philippe Morency. Multimodal language analysis in the wild: Cmu-mosei dataset and interpretable dynamic fusion graph. In *Proceedings of the 56th Annual Meeting of the Association for Computational Linguistics (Volume 1: Long Papers)*, pages 2236–2246, 2018. [5](#)
- [53] Ying Zeng, Wenjun Yan, Sijie Mai, and Haifeng Hu. Disentanglement translation network for multimodal sentiment analysis. *Information Fusion*, 102:102031, 2024. [3](#)
- [54] Qingyang Zhang, Haitao Wu, Changqing Zhang, Qinghua Hu, Huazhu Fu, Joey Tianyi Zhou, and Xi Peng. Provable dynamic fusion for low-quality multimodal data. In *International conference on machine learning*, pages 41753–41769. PMLR, 2023. [1](#)
- [55] Xiaoheng Zhang, Weigang Cui, Bin Hu, and Yang Li. A multi-level alignment and cross-modal unified semantic graph refinement network for conversational emotion recognition. *IEEE Transactions on Affective Computing*, 15(3): 1553–1566, 2024. [6](#)
- [56] Yiyang Zhou, Chenhang Cui, Jaehong Yoon, Linjun Zhang, Zhun Deng, Chelsea Finn, Mohit Bansal, and Huaxiu Yao. Analyzing and mitigating object hallucination in large vision-language models. *arXiv preprint arXiv:2310.00754*, 2023. [1](#)
- [57] Ying Zhou, Xuefeng Liang, Han Chen, Yin Zhao, Xin Chen, and Lida Yu. Triple disentangled representation learning for multimodal affective analysis. *Information Fusion*, 114: 102663, 2025. [6](#)
- [58] Tinghui Zhu, Qin Liu, Fei Wang, Zhengzhong Tu, and Muhao Chen. Unraveling cross-modality knowledge conflicts in large vision-language models. *arXiv preprint arXiv:2410.03659*, 2024. [1](#), [2](#)